Centrosome docking at the immunological synapse is controlled by Lck signaling

Andy Tsun,[1] Ihjaaz Qureshi,[2] Jane C. Stinchcombe,[1] Misty R. Jenkins,[1] Maike de la Roche,[1] Joanna Kleczkowska,[2] Rose Zamoyska,[2,3] and Gillian M. Griffiths[1]

[1]Cambridge Institute for Medical Research, Addenbrooke's Hospital, University of Cambridge, Cambridge CB2 0XY, England, UK
[2]Division of Immune Cell Biology, National Institute for Medical Research, London NW7 1AA, England, UK
[3]Institute of Immunology and Infection Research, University of Edinburgh, Edinburgh EH9 3JT, Scotland, UK

Docking of the centrosome at the plasma membrane directs lytic granules to the immunological synapse. To identify signals controlling centrosome docking at the synapse, we have studied cytotoxic T lymphocytes (CTLs) in which expression of the T cell receptor–activated tyrosine kinase Lck is ablated. In the absence of Lck, the centrosome is able to translocate around the nucleus toward the immunological synapse but is unable to dock at the plasma membrane. Lytic granules fail to polarize and release their contents, and target cells are not killed. In CTLs deficient in both Lck and the related tyrosine kinase Fyn, centrosome translocation is impaired, and the centrosome remains on the distal side of the nucleus relative to the synapse. These results show that repositioning of the centrosome in CTLs involves at least two distinct steps, with Lck signaling required for the centrosome to dock at the plasma membrane.

Introduction

Cytotoxic T lymphocytes (CTLs) destroy virally infected and tumorigenic cells by polarized secretion of lytic granules. Secretion occurs within the immunological synapse formed between CTLs and their target (Stinchcombe et al., 2001). The centrosome plays an important role in directing secretion to this site by contacting the plasma membrane (referred to as docking) and identifying the point of secretion (Stinchcombe et al., 2006). Lytic granules move along microtubules in a minus-end direction toward the centrosome (which is the microtubule-organizing center [MTOC] within CTLs) and are delivered to the plasma membrane at the point determined by the centrosome. Our previous experiments have shown that the centrosome contacts the plasma membrane at the edge of the central supramolecular activation complex (SMAC [cSMAC]), where T cell receptor (TCR) signaling takes place (Stinchcombe et al., 2006). The centrosome is exquisitely sensitive and able to polarize in response to very low avidity signals via the TCR (Jenkins et al., 2009).

Centrosome positioning is important in cell polarity in many different cell types, with the centrosome assuming specific positions in migrating fibroblasts and epithelial and neuronal cells. For example, in migrating fibroblasts, the centrosome relocates to the front of the nucleus toward the leading edge of the cell (Kupfer et al., 1982; Gomes et al., 2005), whereas in migrating neurons, the centrosome is positioned between the leading edge of the cell and the nucleus (Bellion et al., 2005). In migrating T cells, the centrosome has the opposite orientation, between the nucleus and uropod, at the trailing edge of the cell (Dustin et al., 1997; Ratner et al., 1997). What is distinctive about T cells is the ability to polarize the centrosome right up to the plasma membrane during synapse formation (Stinchcombe et al., 2006). Centrosome docking at the plasma membrane is unusual, having previously been observed only during cilia and flagella formation and cytokinesis, when the centrosome contacts the plasma membrane via appendages on the mother centriole (Bornens, 2008).

The signals that control centrosome docking at the synapse in CTLs are not known. Engagement of the TCR triggers a

R. Zamoyska and G.M. Griffiths contributed equally to this paper.

Correspondence to Gillian M. Griffiths: gg305@cam.ac.uk

Abbreviations used in this paper: cSMAC, central SMAC; CTL, cytotoxic T lymphocyte; dSMAC, distal SMAC; ERK, extracellular signal-regulated kinase; MTOC, microtubule-organizing center; PE, phycoerythrin; pSMAC, peripheral SMAC; SMAC, supramolecular activation complex; TCR, T cell receptor; WT, wild type.

The Rockefeller University Press $30.00
J. Cell Biol. Vol. 192 No. 4 663–674
www.jcb.org/cgi/doi/10.1083/jcb.201008140

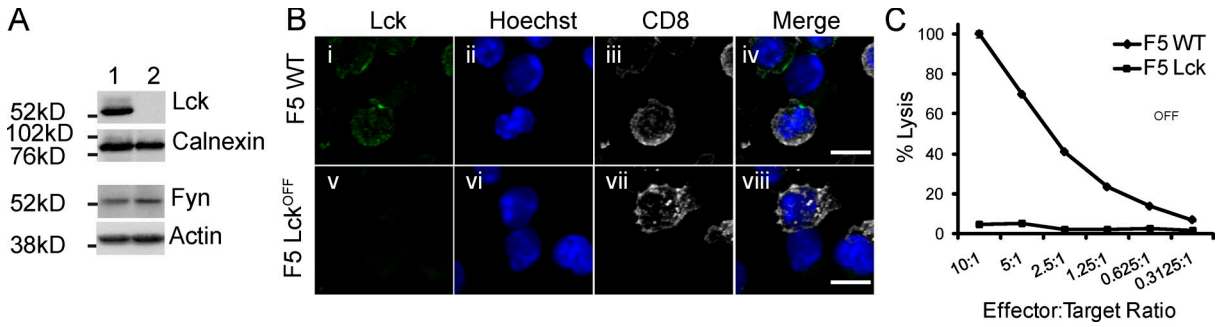

Figure 1. **F5 Lck^{off} CTLs lack killing ability.** (A) Western blot of CTL lysates (7 d after stimulation) for F5 WT (1) and Lck^{off} (2) CTLs probed with antibodies as shown. (B) Immunofluorescence images displaying flattened z stacks of conjugated F5 WT and Lck^{off} CTLs with NP68-pulsed EL4 targets labeled for Lck (green, i and v), nuclei (blue, ii and vi), and CD8 (white, iii and vii). (C) Killing assay of WT (diamonds) and Lck^{off} (squares) F5 CTLs using NP68-pulsed EL4 as targets. Error bars show standard deviation from the means of triplicates. The assay is representative of over three independent experiments. Also see Fig. S1. Bars, 10 µm.

signaling cascade in which Lck and Fyn are two of the first kinases to be recruited. Previous studies examined the roles of signaling proteins in the relocation of the MTOC from the uropod to the synapse side of T cells but did not ask whether the centrosome contacts the plasma membrane. Fyn (Martín-Cófreces et al., 2006), Lck (Lowin-Kropf et al., 1998), LAT, ZAP-70 and Slp76 (Dumont et al., 2002; Kuhné et al., 2003), and DAG production (Quann et al., 2009) have all been implicated in MTOC translocation toward the synapse in CD4 cells. Results from these studies gave some conflicting results, with Lck and ZAP-70 required for MTOC translocation with some stimuli and cell lines but not others (Lowin-Kropf et al., 1998; Blanchard et al., 2002; Kuhné et al., 2003; Martín-Cófreces et al., 2006). Many of these studies took advantage of the Jurkat T cell line and variants produced by ethyl methane sulfate mutagenesis (Weiss and Stobo, 1984). Subsequently, the cell lines used in many of these studies were shown by Western blotting to express undetectable levels of endogenous Fyn (Denny et al., 2000), raising the possibility that lack of Fyn signaling in addition to the protein being investigated contributed to the phenotype. More importantly, these studies predated our observations that lytic granule secretion from CTLs is directed by centrosome docking at the cSMAC of the immunological synapse (Stinchcombe et al., 2006) and can be triggered by very low doses of the antigen (Jenkins et al., 2009). We therefore set out to examine the signals required to control centrosome docking at the cSMAC on the plasma membrane of the immunological synapse.

The first signaling molecules to be activated upon TCR engagement are the Src family tyrosine kinases Lck and Fyn. Lck associates with the cytoplasmic domains of the coreceptors CD8 (or CD4), which associate with the TCR upon binding peptide–major histocompatibility complex. This engagement activates Lck, leading to the phosphorylation of immunoreceptor tyrosine-based activation motif residues in CD3 polypeptides associated with the TCR and the recruitment and activation of the downstream signal cascade. In the absence of Lck, TCR signaling is compromised. Lck-null mice have a block in thymus differentiation and lack mature CD8 and CD4 T cells (Zamoyska et al., 2003). This block can be overcome by an inducible expression of Lck under the control of a tetracycline-responsive promoter in the presence of a T cell–specific trans-activator and doxycycline. Removal of doxycycline results in the loss of Lck expression (Legname et al., 2000). The absence of Lck leads to a profound reduction in phosphorylation of ZAP-70, PLC-γ1, Slp76, and Shc (Lovatt et al., 2006; Salmond et al., 2009). Ca^{2+} signaling is severely reduced, but Akt and extracellular signal-regulated kinase (ERK) phosphorylation and some sites of LAT phosphorylation are less severely affected. These residual signals are mediated by Fyn, which can compensate, to some extent, for the absence of Lck (Lovatt et al., 2006).

Lck-inducible mice have been crossed to TCR transgenic mice (F5) that recognize the influenza-specific peptide NP68 bound to major histocompatibility complex class I (H-2D^{b}), making it possible to study antigen-specific responses. Using this system, we have examined centrosome polarization and lytic granule release from CTLs in an antigen-specific response. We find that, in the absence of Lck, CTLs lose the ability to kill targets. Surprisingly, the centrosome is still able to translocate around the nucleus to face the synapse in cells lacking Lck, and this movement is only blocked when Lck and Fyn are both absent. When Lck alone is deficient, the translocated centrosome remains proximal to the synapse but does not reach the plasma membrane. The killing defect in the absence of Lck lies in the inability of the centrosome to dock at the plasma membrane and deliver lytic granules to the immunological synapse.

Results

CTL-mediated killing is severely impaired in Lck-deficient cells

To examine the signals that control centrosome relocation during the formation of the immunological synapse in T cells, we first examined the role of the proximal tyrosine kinase Lck. We isolated CTLs from F5 TCR transgenic mice, which respond to the NP68 antigenic peptide, with Lck expressed under the doxycycline-inducible promoter so that T cells could develop normally (Legname et al., 2000). Doxycycline was removed 7 d before T cells were isolated. Lck^{off} CTLs were then generated with 10-fold higher doses of the NP68 peptide in vitro compared with wild type (WT) to compensate for reduced levels of Lck protein at the time of activation (Filby et al., 2007). Using these conditions, we were able to generate CTLs in which Lck was ablated.

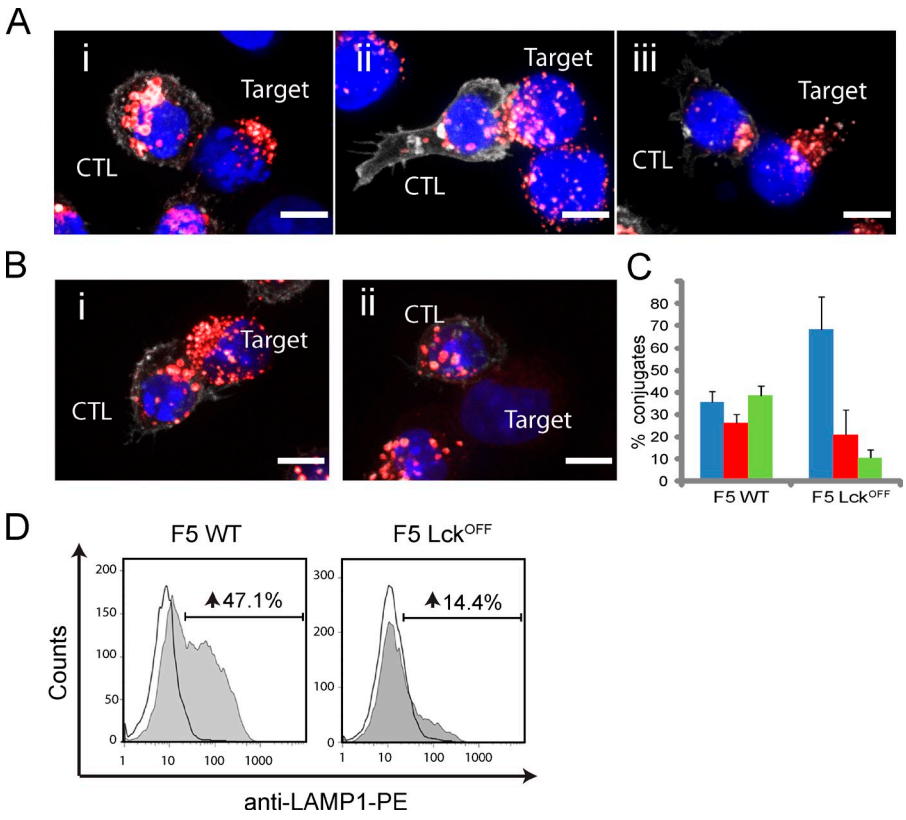

Figure 2. **Lck is essential for degranulation and lytic granule polarization toward the immunological synapse.** (A) Merged immunofluorescence images of three lytic granule polarization phenotypes seen in F5 CTL conjugates with lytic granules: (i) >90% of granules distal, (ii) dispersed, or (iii) tightly clustered at the synapse. Conjugates are labeled with antibodies against LAMP1 (red) or CD8 (white). Nuclei are stained with Hoechst (blue). (B) Representative images of granule polarization observed in (i) WT and (ii) Lck^{off} F5 CTL conjugates. (C) Quantitation of granule polarization in F5 WT ($n = 465$) and Lck^{off} ($n = 484$) CTLs for granules that were distal (blue), dispersed (red), or tightly polarized (green) at the immune synapse. Error bars show the standard deviation from the means of at least three independent experiments. A two-tailed Student's *t* test for loss of granule polarization in Lck^{off} samples compared with WT gave a statistical significance of $P = 5 \times 10^{-6}$. (D) Histograms of a CTL degranulation assay displaying a $CD8^+$ cell count against a LAMP1-PE signal upon activation with pulsed (shaded) or unpulsed (unshaded) EL4 targets. The percent increase in LAMP1 staining with a pulsed versus an unpulsed target is given. Data are representative of more than three independent experiments. Bars, 5 µm.

Lck^{off} CTLs differentiated normally with equivalent levels of granzymes A and B and perforin as well as the equivalent expression of activation markers CD69, CD25, CD44, CD62L, and CD11a compared with F5 WT CTLs (Fig. S1).

Lck mRNA was not detected (unpublished data), and protein was undetectable in Lck^{off} CTLs (Fig. 1 A). Expression in single cells, analyzed by immunofluorescence (Fig. 1 B), showed that Lck clustered to form the cSMAC in 44% of all F5 WT conjugates with peptide-pulsed EL4 targets, with no expression seen in almost all Lck^{off} CTLs. Very low levels of residual Lck could occasionally be detected in individual Lck^{off} CTLs visible only when clustered at the synapse of conjugates (<10%), suggesting that very low levels of residual protein occasionally remained in isolated CTLs. Lck^{off} CTLs formed conjugates with peptide-pulsed EL4 targets as effectively as WT CTLs, with 25% of CTLs forming conjugates in each case ($n > 3{,}000$). However, the killing of peptide-pulsed targets by Lck^{off} was severely impaired compared with killing by F5 WT CTLs (Fig. 1 C). These results show that loss of Lck results in loss of CTL-mediated killing, even though Lck^{off} CTLs express all of the lytic granule proteins required for killing and, upon re-expression of Lck in vivo, are capable of killing targets (unpublished data).

Granule polarization and degranulation are defective in Lck-deficient CTLs

To identify the stage at which secretion was blocked in Lck^{off} CTLs, we first examined whether the lytic granules were able to polarize to the immune synapse in Lck^{off} CTLs when forming conjugates with peptide-pulsed EL4 targets (Fig. 2 A). Conjugates were fixed and stained with antibodies against CD8 (Fig. 2 A, white) and LAMP1 (CD107a; Fig. 2 A, red), with Hoechst to stain the nuclei. Although 39% of conjugates ($n = 465$) from F5 WT showed the majority of granules tightly clustered at the synapse, this phenotype was only observed in 11% of F5 Lck^{off} conjugates ($n = 484$), demonstrating that granule polarization is impaired in the absence of Lck (Fig. 2, B and C).

We assessed the ability of Lck-deficient CTLs to release lytic granules using uptake of anti–LAMP1-phycoerythrin (PE) by CD8 cells to monitor granule release at 30 min (Fig. 2 D). This assay revealed that although 47.1% of F5 WT CTLs took up LAMP1 in response to peptide pulse compared with unpulsed targets, only 14.4% of Lck^{off} CTLs did so. The low level of granule polarization and release is consistent with the low level of residual Lck occasionally detected. These results show that both granule polarization and degranulation are defective in Lck-deficient CTLs.

Lck is required for docking of the centrosome at the plasma membrane

Our previous experiments have revealed a correlation between the formation of the distal SMAC (dSMAC) and the docking of the centrosome at the plasma membrane (Stinchcombe et al., 2006). We examined the position of the centrosome in F5 WT and Lck^{off} CTLs. Conjugates formed between WT and Lck^{off} CTLs with peptide-pulsed EL4 targets were fixed and labeled with antibodies against CD8 (Fig. 3 A, white) to identify the T cell, talin (Fig. 3 A, green) to identify the peripheral SMAC (pSMAC), and γ-tubulin (Fig. 3 A, red) to identify the centrosome. Nuclei were stained with Hoechst dye, and the position of the

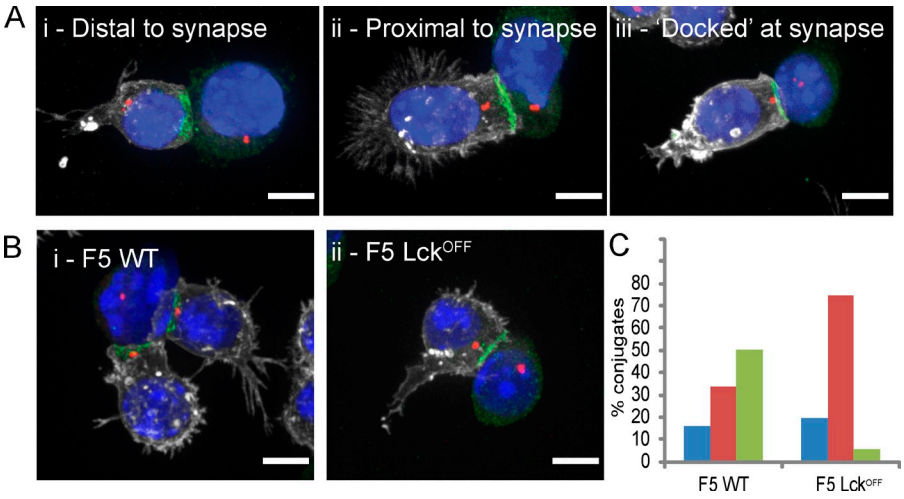

Figure 3. **Lck is required for complete polarization and docking of the centrosome to the immunological synapse.** (A) Merged immunofluorescence projections of centrosome polarization phenotypes seen in F5 CTL conjugates with the centrosome distal, proximal, or docked at the synapse (i.e., with γ-tubulin contacting the plasma membrane marker CD8), with cells labeled with antibodies against talin (green), γ-tubulin (red), and CD8 (white). Nuclei are stained with Hoechst (blue). (B) Representative images of centrosome polarization observed in WT and Lck^{off} CTLs. Every image (A and B) is a merge of four channels collected from z stacks. (C) Quantitation of centrosome polarization for F5 WT (n = 112) and F5 Lck^{off} (n = 103) from data analyzed in 3D showing the percentage of conjugates with the centrosome distal (blue), proximal (red), or docked (green) at the synapse. A two-tailed Student's t test for loss of centrosome docking in Lck^{off} samples compared with WT gave a statistical significance of $P = 10^{-4}$. Centrosome polarization was also quantitated in three independent experiments without 3D reconstruction (Fig. S3). Bars, 5 µm.

centrosome was classified according to whether the signal given by γ-tubulin was on the distal or proximal side of the nucleus relative to the synapse or docked (i.e., in contact) with the plasma membrane marker CD8 (Fig. 3 A). All images were collected as z stacks and reconstructed using Volocity software so that they could be viewed in 3D to accurately classify the position of the centrosome relative to the synapse and the nucleus.

The centrosome was docked at the plasma membrane of the immune synapse in 50% of conjugates formed between F5 WT CTLs and targets. The centrosome was on the synapse-proximal side of the nucleus, but not docked, in 34% of conjugates and on the distal side of the nucleus from the synapse in the remaining 16% of conjugates (n = 112; Fig. 3, B and C; and Video 5). In Lck^{off} CTLs, the position of the centrosome was different. In 75% of the conjugates formed by Lck^{off} CTLs, the centrosome was found to be proximal to the synapse but not docked at the plasma membrane (Fig. 3, B and C; and Video 6). The centrosome was only docked at the plasma membrane in 6% of conjugates and remained on the distal side of the nucleus relative to the synapse in the remaining 19% of conjugates (n = 103).

These results show that centrosome polarization to the synapse is impaired in Lck^{off} CTLs. Although WT CTLs docked the centrosome at the synapse efficiently, Lck^{off} CTLs were unable to do so, and instead, the centrosome repositioned only as far as the synapse side of the nucleus (Fig. 3 C). Because docking of the centrosome precedes granule polarization in mouse CTLs (Jenkins et al., 2009), the loss of centrosome docking in Lck^{off} CTLs will lead to the loss of granule delivery to the synapse and an inability to kill targets.

Centrosome relocation is impaired in Lck-deficient CTLs

To understand the unusual positioning of the centrosome in Lck^{off} CTLs, we used EM to examine centrosome positioning in unconjugated CTLs and CTLs forming synapses with target cells. In unconjugated CTLs, which have the morphology of rounded nonmotile cells, the two centrioles of the centrosome appeared to be associated with the nucleus. The centrosome was often seen next to a small invagination in the nuclear structure (Fig. 4 A), with the MTOC, and associated organelles radiated out from the centrosome. The lytic granules were distributed along microtubules throughout the cell. Unconjugated CTLs with migratory morphologies show a distinctive leading edge and uropod (Fig. 4 B). In these CTLs, the centrosome was seen in the uropod, displaced from the nucleus by some distance, as previously noted in low resolution experiments (Ratner et al., 1997). Microtubules and MTOC-associated organelles radiated out from the centrosome, and the lytic granules were distributed along microtubules throughout the cell. No differences were apparent between unconjugated F5 WT and Lck^{off} CTLs.

Upon interaction with targets, T cells receive a stop signal, and the cells round up as they form conjugates (Negulescu et al., 1996; Dustin et al., 1997). This was apparent in EM images from both WT and Lck^{off} CTLs (Fig. 4 C). In EM images of WT CTLs, the centrosome was often in contact with the plasma membrane, which we refer to as docking, and was separated from the nuclear envelope. The MTOC and associated organelles radiated out from this point and had the appearance of streaming toward the point of centrosome contact with the plasma membrane (docking). Lytic granules also focused toward the point of centrosome contact at the plasma membrane. All of these organelles appeared to be aligned along microtubules, which converged at the centrosome (Fig. 4 C, WT).

In EM images of conjugates formed by F5 Lck^{off} CTLs, the centrosome was located between the nucleus and the synapse but was not in contact with the plasma membrane (Fig. 4 C). The centrosome appeared closer to the nucleus than in WT conjugates, although not as close as in the rounded nonmigratory cells (Fig. 4 A). The microtubule-associated organelles radiated out from the centrosome but lacked the streaming organization seen in WT CTL conjugates, with lytic granules dispersed throughout the cell (Fig. 4 C, Lck^{off}).

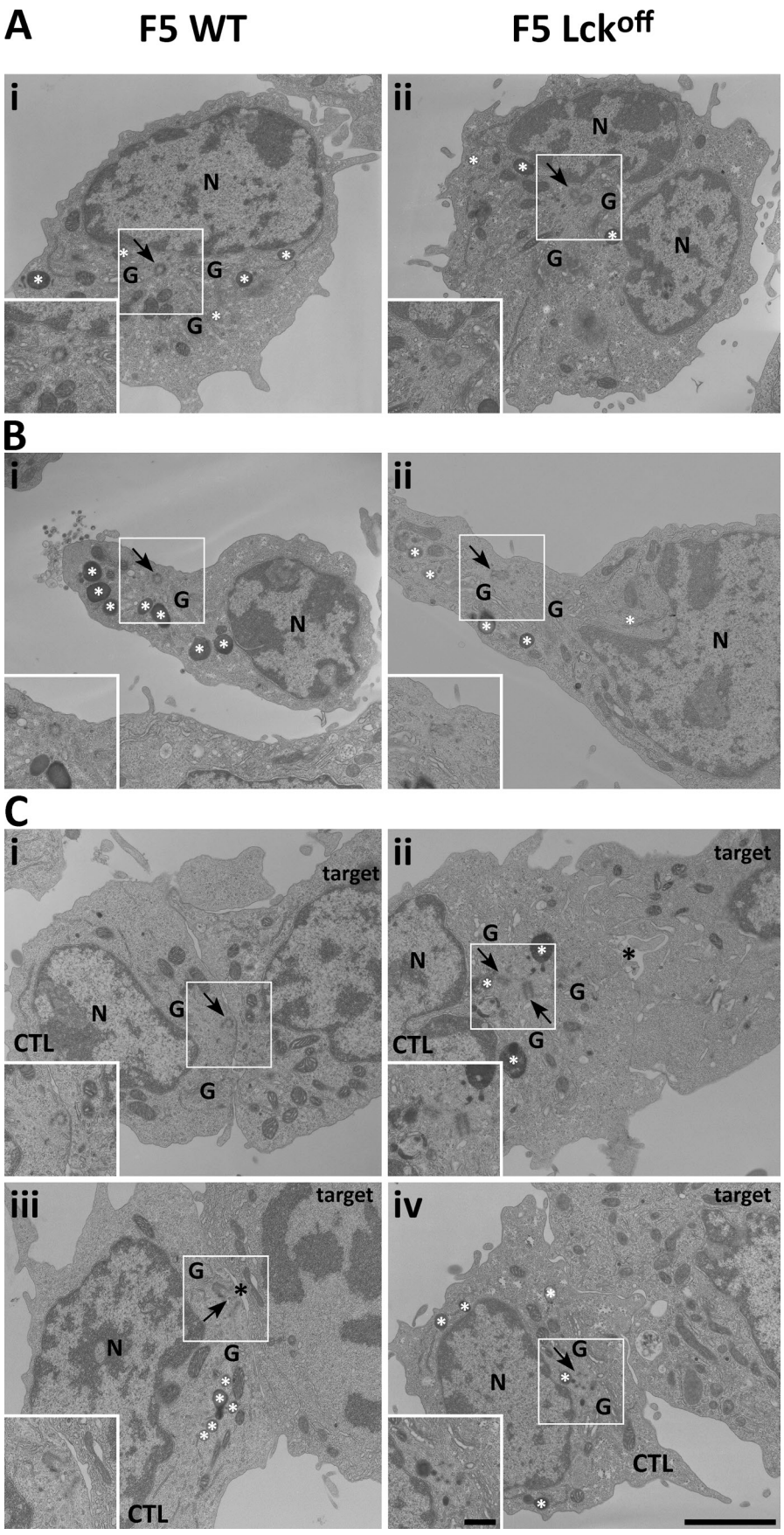

Figure 4. **The centrosome fails to dock at the immunological synapse in Lck^{off} CTLs.** (A–C) EM micrographs from thin (50–100 nm) lead-stained sections of nonmotile (A), motile (B), and target-conjugated (C) F5 WT or Lck^{off} CTLs loaded with HRP to reveal the endocytic pathway. The Golgi complex (G), lytic granules (white asterisks), secretory cleft (black asterisks), nuclei (N), and centrosome (arrows) are indicated in each image. Insets are magnified images of the centrosome area marked by white boxes. Bars: (main panels) 2 µm; (insets) 0.5 µm.

Table I. **Quantitation of electron micrographs of conjugates formed between F5 WT or Lck^{off} CTLs with NP68-pulsed EL4 target cells**

Time point	Proximal percentage	Distal percentage	Docked percentage	*n*
F5 WT CTL				
20 min	10	0	90	11
40 min	15	0	85	27
60 min	10	0	90	10
F5 Lck^{off} CTL				
20 min	80	10	10	10
40 min	81	14	5	21
60 min	89	11	0	19

The number of conjugates analyzed at each time point is given (*n*).

To verify the defect in centrosome docking in Lck^{off} CTLs at a higher resolution, we quantitated centrosome docking at the plasma membrane from electron micrographs prepared from samples in which CTLs were allowed to conjugate for 20, 40, or 60 min. Only sections in which at least one of the centrioles and a clear synapse were seen were counted. Centrioles have approximate dimensions of 0.45 × 0.2 µm. The centrosome was classified as being docked when one centriole was within 0.5 µm of the plasma membrane and proximal if it was further than 0.5 µm from the plasma membrane but still on the synapse side of the nucleus. When the centrosome was observed on the far side of the nucleus relative to the synapse, it was classified as distal. Using these criteria, the centrosome was found to be proximal to the synapse in 10–15% of conjugates and docked in 85–90% of conjugates formed using F5 WT CTLs, whereas the centrosome remained proximal to the synapse in 70–89% of conjugates formed by F5 Lck^{off} CTLs and was only found to be docked in 10–14% at the different time points examined (Table I).

These numbers are consistent with the quantitation of centrosome positioning obtained from the immunofluorescence images (Fig. 3 C) in revealing the loss of centrosome docking in the absence of Lck. It is important to remember that EM images are derived from thin sections (50–100 nm) of cells compared with immunofluorescence images in which the entire depth of the cell can be viewed. Because EM images were selected to show the centrioles and synapse in the same section, images in which the centrosome might have been distal or even sometimes proximal to the synapse relative to the nucleus were inevitably under represented. What these images reveal is the difference in centrosome positioning close to the synapse between WT and Lck^{off} CTLs, with Lck^{off} CTLs failing to bring the centrosome next to the plasma membrane at the synapse. The loss of centrosomal docking at the plasma membrane of conjugates formed by F5 Lck^{off} CTLs correlates with the loss of target cell killing (Fig. 1 A), demonstrating the need for centrosomal docking for granule delivery and CTL-mediated killing.

Actin reorganization at the immunological synapse is impaired in Lck-deficient CTLs

Our previous studies have demonstrated a correlation between the clearance of actin and centrosome docking at the plasma membrane (Stinchcombe et al., 2006). Actin initially accumulates across the interface of the synapse (Ryser et al., 1982; Kupfer et al., 1994) into the peripheral ring (Stinchcombe et al., 2001, 2006), which forms the dSMAC (Freiberg et al., 2002). We therefore asked whether actin clearance was disrupted in Lck-deficient CTLs. By staining F5 WT and Lck^{off} CTL conjugates for actin and examining these by 3D confocal microscopy, we were able to visualize the dSMAC ring of actin in 58% (n = 121) of conjugates formed by F5 WT CTLs. However, in conjugates formed by F5 Lck^{off} CTLs, the actin dSMAC was only found in 22% of conjugates (n = 110), with the remainder only partially reorganizing actin or failing to do so (Fig. 5, A and B; and Videos 1 and 2).

Because dSMAC organization was disrupted, we asked whether pSMAC formation was affected by the loss of Lck by examining staining with talin, the cytosolic protein that associates with integrins forming the ring of the pSMAC in the immunological synapse. Talin staining revealed the characteristic ring of the pSMAC in 47% (n = 117) of conjugates formed by F5 WT CTLs, but the pSMAC ring could only be seen in 20% (n = 119) of conjugates formed by Lck^{off} CTLs (Fig. 5, C and D; and Videos 3 and 4). These results indicate that Lck signaling is required for the clearance of actin and talin into the dSMAC and pSMAC regions of the synapse, respectively. Loss of actin clearance correlates with the loss of centrosome movement to the plasma membrane and is consistent with a model in which actin reorganization into the dSMAC generates forces that pull the centrosome forward to the plasma membrane from a site proximal to the synapse (Stinchcombe et al., 2006).

TCR and non-TCR signals can trigger centrosomal translocation relative to the nucleus

We were struck by our finding that, in the absence of Lck-mediated signals, the centrosome was nevertheless able to translocate around the nucleus toward the synapse. Centrosome localization plays a key role in cell polarity in nonimmune cell types, and the centrosome is able to polarize around the nucleus in response to wound healing in fibroblast cells in the absence of TCR-activated signaling. For this reason, we wanted to know whether TCR-mediated and non-TCR–mediated signals were able to trigger the centrosome repositioning that we observed in Lck-deficient CTLs.

To provide only TCR signaling to the CTLs, we used latex beads coated with antibodies to the CD3 subunit of the TCR. CTLs were allowed to form conjugates with beads for 20 min before being fixed and labeled with antibodies to γ-tubulin

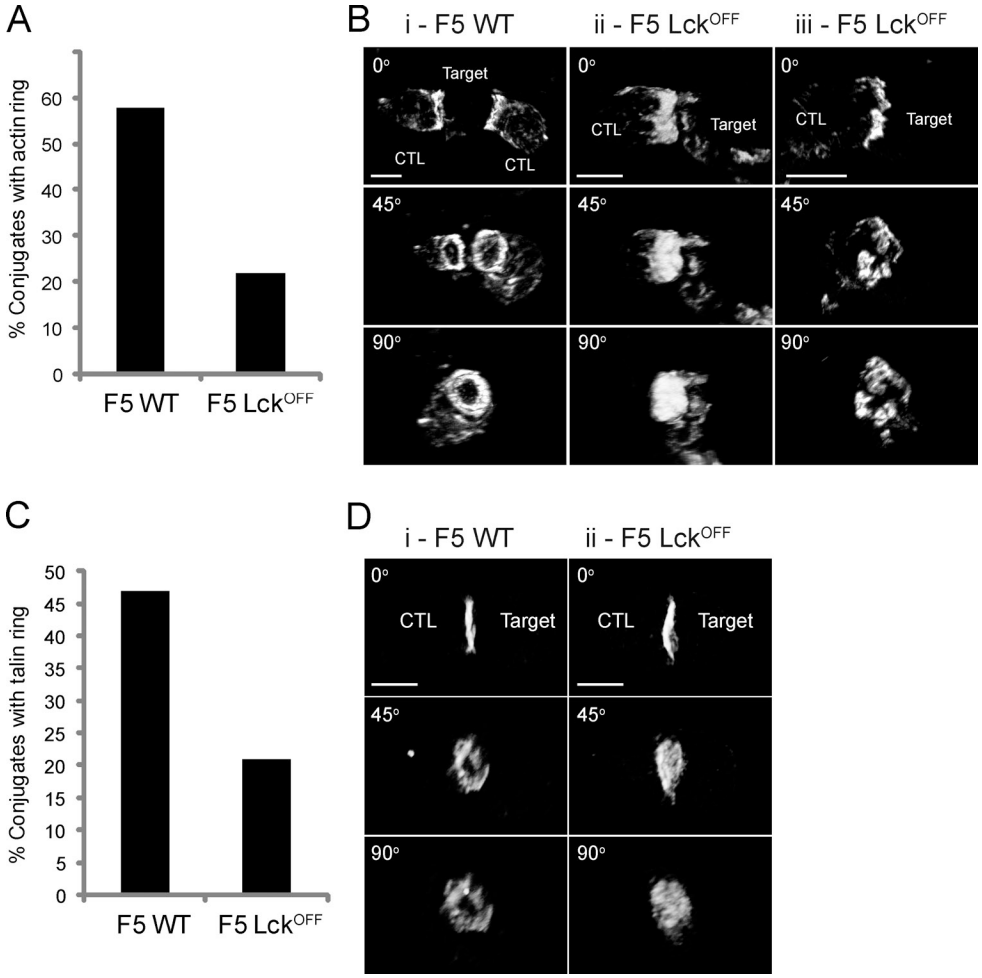

Figure 5. **Actin clearance into the dSMAC is impaired in the absence of Lck F5 WT and Lck^{off} CTL conjugates with NP68-pulsed EL4 targets.** (A) Quantitation of forming dSMACs from 3D reconstructions labeled for actin (WT, *n* = 121 and Lck^{off}, *n* = 110). (B) Representative 3D images of actin staining in WT and Lck^{off} CTLs in which actin has failed to clear (ii) or has partially reorganized (iii). (C) Quantitation from 3D reconstructions (WT, *n* = 117 and Lck^{off}, *n* = 119). (D) 3D images for pSMACs labeled for talin at the synapse. All 3D images are displayed at 0, 45, and 90° rotations. Bars, 10 µm.

(Fig. 6 B, red). The nucleus was stained with Hoechst (Fig. 6 B, blue). The position of the centrosome relative to the bead was then scored as proximal or distal (Fig. 6 A). Quantitation of the bead conjugates revealed that 78% of WT and 72% of Lck^{off} CTLs polarized the centrosome toward the CD3-coated bead. In the presence of the tyrosine kinase inhibitor PP2, only 24% of bead conjugates were able to reposition the centrosome toward the bead (Fig. 6 C). These results show that TCR signaling alone can mediate polarization of the centrosome to the proximal side of the nucleus in the presence or absence of Lck. However, ablation of additional Src family tyrosine kinase activity with PP2 abolished the ability of the centrosome to translocate around the nucleus to face the bead.

We also asked whether non-TCR–mediated signals might also trigger centrosomal translocation in T cells. We therefore compared centrosome polarization in CTLs using anti-CD3–coated beads coated with antibodies to the integrin chain CD11a, the coreceptor CD28, and the transferrin receptor. Anti-CD3–coated beads gave similar results to those in Fig. 6 C, with 74% of conjugates showing the centrosome proximal to the bead compared with background levels of 18% with beads coated with antitransferrin receptor antibodies. Both cross-linking of CD11a (48%) and CD28 (39%) elicited centrosome translocation to the bead-proximal side of the nucleus above background levels (Fig. 6 D), which was consistent with previous observations in CD4 cells (Sedwick et al., 1999; Barnard et al., 2005; Nejmeddine et al., 2009). This demonstrates that centrosome translocation can be triggered by both TCR and non-TCR signaling pathways in CTLs.

Lck and Fyn are required for centrosomal polarization around the nucleus

The observation that PP2 could inhibit centrosomal translocation in Lck^{off} CTLs indicated that additional tyrosine kinases contributed to centrosome translocation toward the synapse. The tyrosine kinase Fyn is also expressed in CD8 cells and is dispensable for CTL differentiation, providing Lck is expressed. Fyn-deficient CTLs kill targets effectively (Filby et al., 2007). However, like F5 Lck^{off} CTLs, Lck^{off} Fyn$^{-/-}$ CTLs are unable to kill targets (Fig. 7 A) even though they are activated and express perforin and granzymes A and B

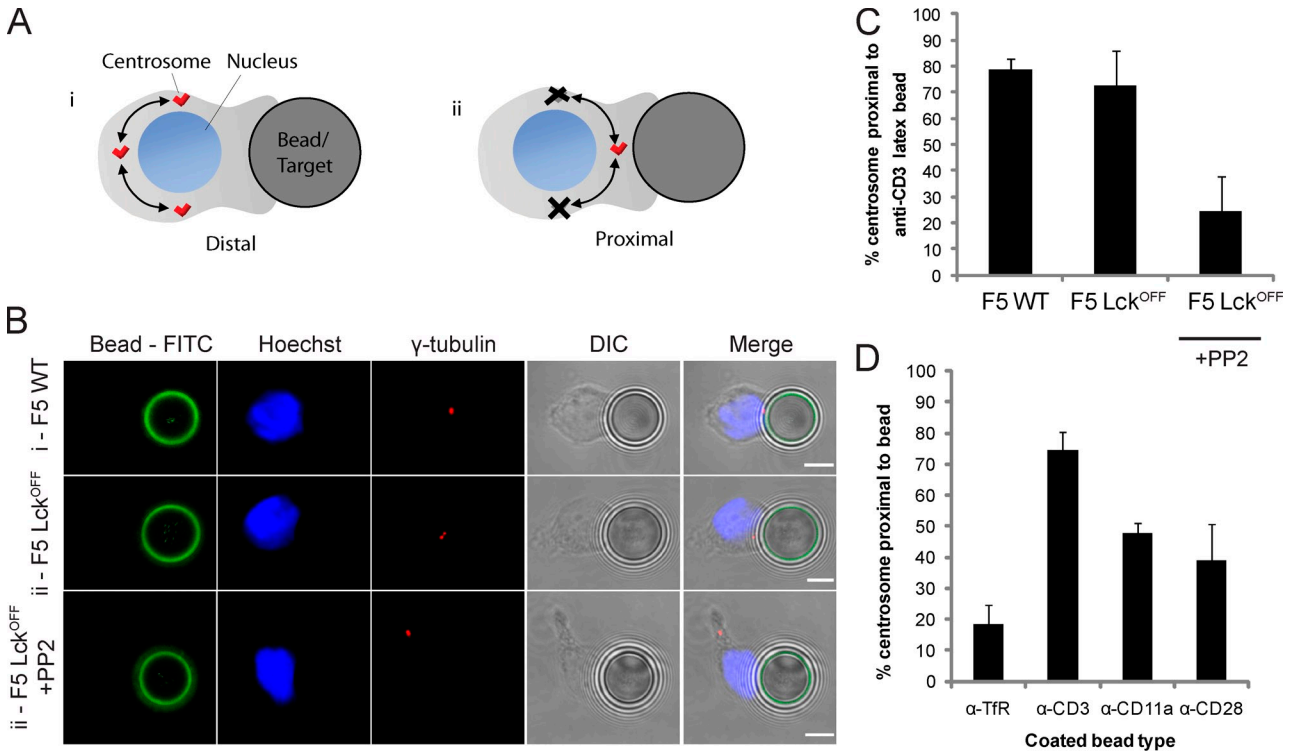

Figure 6. **Lck-deficient CTLs can polarize their centrosome toward antigen-presenting targets or anti-CD3 beads.** (A) Cartoon defining distal and proximal positions of the centrosome relative to beads or targets. (B) Representative images of conjugates formed between rat anti-CD3 latex beads and F5 CTLs from WT, Lck^{off}, and Lck^{off} + PP2 labeled with antibodies to γ-tubulin (red) and anti–rat-FITC (green) in separate channels, viewed by differential interference contrast (DIC), and merged. (C) Quantitation of conjugates from F5 WT (n = 400), Lck^{off} (n = 400), or Lck^{off} + PP2 inhibitor (n = 300) CTL conjugates. A two-tailed Student's t test for differences between WT and Lck^{off} samples + PP2 revealed a statistical significance (P = 0.01). (D) Quantitation of centrosome polarization from OT-I CTL-bead conjugates. Error bars show the standard deviation from the means from at least three independent experiments. n > 300 conjugates. Bars, 5 µm.

at WT levels (Fig. S1). We therefore asked whether centrosome polarization was defective in Lck^{off} Fyn$^{-/-}$ CTLs and whether there was any difference with the defect seen in Lck^{off} CTLs. Conjugates generated with peptide-pulsed EL4 target cells were analyzed as part of the same experiment shown in Fig. 3. The defect seen in Lck^{off} Fyn$^{-/-}$ CTLs was distinct from that seen in Lck^{off} CTLs (Fig. 7 B). The centrosome remained on the distal side of the nucleus relative to the synapse in 61% of conjugates and on the synapse-proximal side of the nucleus in 28% of conjugates and was only docked at the plasma membrane in 11% of conjugates (n = 103; Fig. 7 C and Video 7). These results demonstrate that, when both Fyn and Lck are lost, centrosomal translocation toward the synapse is impaired.

We asked whether Fyn was responsible for the PP2-inhibitable residual Src kinase activity required for centrosome polarization, which we observed in Fig. 6 C. Using anti-CD3–coated beads to trigger TCR signaling, we found that Lck^{off} Fyn$^{-/-}$ CTLs were unable to polarize the centrosome around the nucleus toward the bead, with the centrosome remaining distal in 60% of conjugates (Fig. 7 D). This number of conjugates in which the centrosome was able to reposition toward the bead was not significantly changed by the addition of PP2, suggesting that other kinases play only a minor role, if any.

Discussion

Centrosome polarization toward the immunological synapse plays an important role in directing polarized secretion from T cells (Geiger et al., 1982; Kupfer et al., 1983; Kupfer and Dennert, 1984). Our own experiments have shown that the centrosome not only polarizes toward but also contacts the plasma membrane within the synapse (Stinchcombe et al., 2006), determining the point of lytic granule secretion. In this study, we examine the signals required for centrosome docking. We find that, in the absence of Lck signaling, the centrosome is able to translocate from the rear of the cell around the nucleus toward the synapse. However, the centrosome is no longer able to dock at the plasma membrane.

Previous studies have indicated that Lck, Fyn, LAT, ZAP-70, and Slp76 were all involved in the translocation of the centrosome from the rear of the cell toward the synapse (Lowin-Kropf et al., 1998; Blanchard et al., 2002; Kuhné et al., 2003; Martín-Cófreces et al., 2006). The majority of these studies were performed in the CD4 Jurkat cell line, in which it was not possible to study antigen-specific responses. Additionally, the demonstration of extremely low levels of Fyn in Jurkat cell lines used in these studies (Denny et al., 2000) complicated the interpretation, as Fyn was also likely to have been deficient in these cells. Studies in antigen-specific CD4 T cells have made use of

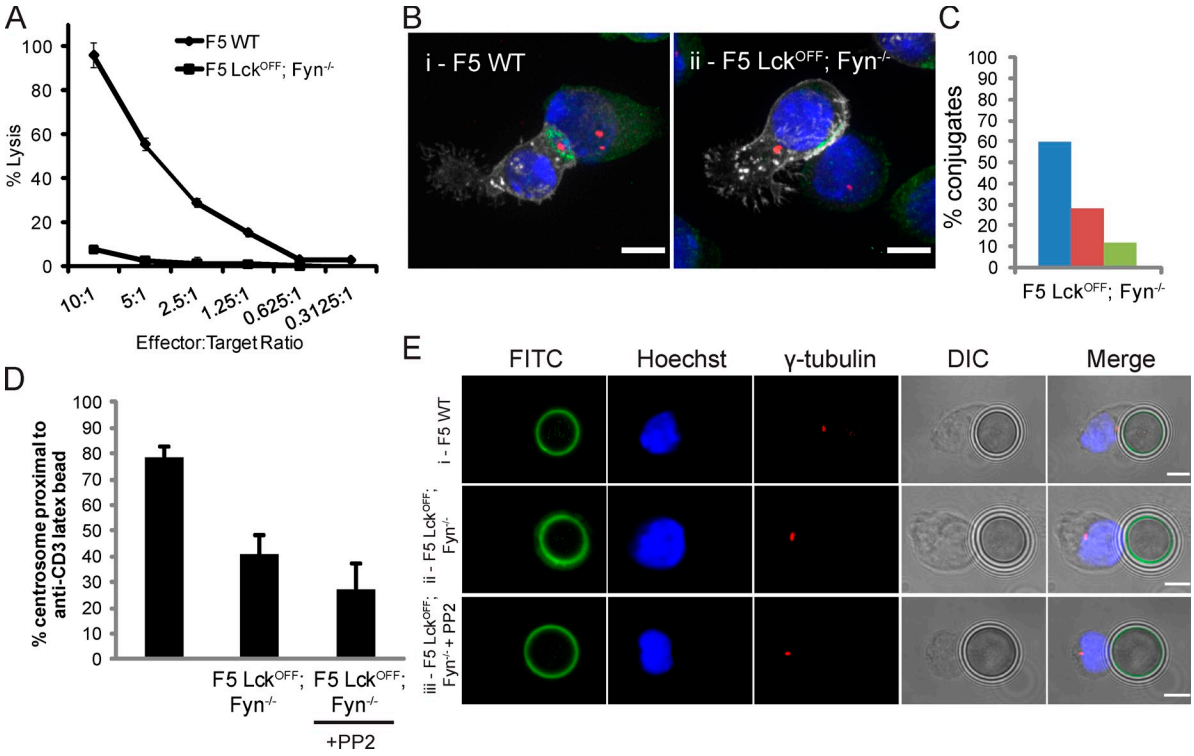

Figure 7. **Lck- and Fyn-deficient CTLs cannot polarize their centrosome toward antigen-presenting targets or anti-CD3 beads.** (A) Killing assay of F5 WT (diamonds) and Lck^{off} Fyn$^{-/-}$ (squares) CTLs using NP68-pulsed EL4 as targets. Error bars show standard deviations from triplicates. (B) Representative immunofluorescence images of centrosome polarization observed in WT and Lck^{off} Fyn$^{-/-}$ F5 CTLs with NP68-pulsed EL4 targets. Cells are labeled with antibodies against talin (green), γ-tubulin (red), and CD8 (white). Nuclei were stained with Hoechst (blue). Bars, 10 µm. (C) Quantitation of centrosome position relative to the synapse in conjugates formed between EL4-pulsed targets and F5 Lck^{off} Fyn$^{-/-}$ (n = 103) CTLs from 3D reconstructions from the same experiment shown in Fig. 3 C showing distal (blue), proximal (red), or docked (green) centrosomes at the synapse. A two-tailed Student's t test for loss of centrosome docking in Lck^{off} samples compared with WT gave a statistical significance of P = 0.007. Lck^{off} Fyn$^{-/-}$ formed conjugates with similar frequency (31%; n = 317) to WT CTLs (33%; n = 424). Centrosome polarization was also quantitated in three independent experiments without 3D reconstruction (Fig. S3). (D) Quantitation of centrosome position relative to anti-CD3 antibody–coated latex beads for F5 WT (n = 400), Lck^{off} Fyn$^{-/-}$ (n = 400), and Lck^{off} Fyn$^{-/-}$ + PP2 (n = 300) CTL conjugates. Error bars show the standard deviation from the means from at least three independent experiments. A two-tailed Student's t test for loss of centrosome docking in Lck^{off} and Lck^{off} Fyn$^{-/-}$ samples compared with WT gave statistical significances of P = 0.0006 and P = 0.007, respectively. (E) Representative images of F5 CTLs from WT, Lck^{off} Fyn$^{-/-}$, and Lck^{off} Fyn$^{-/-}$ + PP2 conjugated to anti-CD3 antibody–coated latex beads labeled with Hoechst (blue) and antibodies against γ-tubulin (red) and anti–rat-FITC (green) viewed by differential interference contrast (DIC) and merged. Also see Fig. S2. Bars, 5 µm.

inhibitors of PLC-γ production (Quann et al., 2009) as well as overexpression of kinase-dead variants of Fyn and Lck (Martín-Cófreces et al., 2006) to perturb the signaling pathways and suggested that all of these effectors play a role in the initial translocation of the centrosome from the rear of the T cell to the synapse. However, none of these studies have examined the signals required for centrosome docking at the plasma membrane.

The generation of mice with Lck under the control of an inducible promoter (Legname et al., 2000) provided an ideal system in which to study centrosome polarization in the absence of Lck alone in an antigen-specific system. Lck is a very long-lived protein, with early experiments showing no reduction in levels of metabolically labeled protein within 24 h (Veillette et al., 1993). We found that it was necessary to remove doxycycline before activation to generate CTLs completely lacking Lck protein. Use of a higher peptide concentration for stimulation compensated for the reduced Lck protein levels at the point of activation and generated CTLs lacking Lck. When we reduced doxycycline for shorter time periods, Lck was detectable by Western blotting, and CTL activity was normal. The CTLs generated were always checked for Lck expression, both by Western blotting and by immunofluorescence to confirm the complete absence of Lck before analysis. We were able to restore degranulation in Lck-depleted cells by nucleofection of Lck-YFP (see Materials and methods), demonstrating that the defect is simply caused by the loss of Lck.

Using this system to generate CTLs lacking only Lck, we found that these cells were able to translocate the centrosome toward the synapse; however, the centrosome failed to reach the plasma membrane. Only in CTLs doubly deficient in both Lck and Fyn was centrosomal translocation, from the rear of the cell to the synapse, impaired.

It was surprising to find that the centrosome polarization was still able to translocate toward the synapse in the absence of Lck, as it is the tyrosine kinase most proximal to TCR. However, although TCR-mediated signaling is compromised in Lck-deficient cells, it is not completely absent. Akt, ERK, and JNK phosphorylation and calcium flux are all reduced but not absent (Fig. S2; Lovatt et al., 2006; Filby et al., 2007; Salmond et al., 2009), and these may provide sufficient signals to trigger the repositioning of the centrosome toward the synapse. By using anti-CD3–coated beads to trigger only via the TCR, we were

able to demonstrate that the residual TCR signaling was sufficient to mediate centrosome repositioning.

In the current study, we find that only CTLs doubly deficient in both Lck and Fyn lose the ability to translocate the centrosome from the rear of the cell, around the nucleus, toward the synapse. Therefore, our results are consistent with previous studies examining the translocation of the MTOC from the rear of the cell toward the synapse (Lowin-Kropf et al., 1998; Martín-Cófreces et al., 2006) when you take into account that the JCaM1 cells deficient in Lck would also have been deficient in Fyn (Denny et al., 2000). These cell lines would, therefore, correspond to the doubly deficient Lck^{off} $Fyn^{-/-}$ CTLs used in our experiments in which centrosomal translocation toward the synapse is inhibited. Our results, which discriminate between Lck and Lck-plus-Fyn signaling, demonstrate that centrosome polarization to the synapse is a multistep process. The centrosome translocates around the nucleus toward the synapse, and then, in a distinct step requiring Lck signaling, the centrosome moves forward to contact the plasma membrane.

The important finding from our experiments is that, although the centrosome translocates toward the synapse in the absence of Lck, it is unable to dock at the plasma membrane. Conjugates formed at 20, 40, and 60 min all reveal a loss of centrosomal docking at the plasma membrane, demonstrating that centrosomal docking at the plasma membrane is lost in the absence of Lck rather than simply being delayed. Furthermore, a 4-h killing assay revealed that Lck-deficient CTLs fail to kill targets even after this prolonged time, supporting the idea that centrosome polarization is not simply delayed in Lck-deficient CTLs. Lck-deficient CTLs also show defects in granule polarization to the synapse. Although the loss of granule polarization in Lck-deficient CTLs may result from reduced signaling in these cells, these results rather support the idea that centrosomal docking itself is a prerequisite for granule delivery to the synapse.

Our EM images indicate that the centrosome is tightly associated with the nucleus in rounded nonmigratory CTLs but positioned some distance from the nuclear envelope in the uropod of migratory T cells. In Lck-deficient CTLs, the centrosome is positioned on the synapse side of the nucleus surrounded by a loose array of MTOC-associated organelles but does not appear to be more closely associated with the nuclear membrane than in WT. This suggests that the loss of centrosomal migration toward the plasma membrane is unlikely to arise from an increased association with the nuclear envelope but rather from the loss of forces required to pull the centrosome up to the plasma membrane.

How might loss of centrosome docking arise in the absence of Lck? One striking difference between WT and Lck^{off} conjugates is that pSMAC and dSMAC formation are impaired, which is consistent with Lck-mediated signaling preceding synapse formation (Lee et al., 2002). In Lck^{off} conjugates, actin accumulates across the synapse but often fails to clear into a dSMAC. These results are reminiscent of the correlation observed between actin clearance into the dSMAC and docking of the centrosome at the plasma membrane previously observed (Stinchcombe et al., 2006). These results support a model of centrosome polarization in which forces generated at the synapse as actin is cleared into the dSMAC bring the centrosome forward to contact the plasma membrane (Stinchcombe and Griffiths, 2007).

The polarization of the centrosome around the nucleus occurs in many nonlymphoid cell types in response to external stimuli, which is distinct from lymphoid antigen receptor engagement. One well-studied example is wound healing in fibroblasts, when centrosome polarization toward the wound is mediated by the rotation of the nucleus within the cell (Gomes et al., 2005) with the centrosome staying fixed relative to the nucleus. Cdc42, actin, and dynein have all been implicated in MTOC polarization in both fibroblasts (Etienne-Manneville and Hall, 2001; Palazzo et al., 2001) and T cells (Stowers et al., 1995; Kuhn and Poenie, 2002; Combs et al., 2006; Stinchcombe et al., 2006), and these mediators are thought to act by controlling nuclear rotation in fibroblasts (Gomes et al., 2005; Levy and Holzbaur, 2008).

We do not know whether the centrosome maintains its position relative to a rolling nucleus or whether the centrosome moves around the nucleus as it approaches the immunological synapse in T cells. However, it is clear that signals for centrosome polarization can be triggered by non-TCR–mediated signals (Fig. 6 D). Anti–ICAM-1–coated beads can trigger MTOC polarization in HTLV1-infected T cells at the virological synapse (Nejmeddine et al., 2009), and E-cadherin has also been shown to be able to trigger centrosome polarization in epithelial cells (Desai et al., 2009). Our experiments suggest that the initial translocation of the centrosome toward the immunological synapse is triggered readily, by multiple and minimal signals. However, the distinctive step in CTLs in which centrosomal docking at the plasma membrane occurs is tightly controlled by the TCR signaling pathway, with Lck playing a key role.

Materials and methods

Antibodies

Mouse antibodies were against actin (AC-40), talin (8D4; Sigma-Aldrich), and Lck (3A5; Millipore) or rabbit antiactin (A2066), γ-tubulin (T5192; Sigma-Aldrich), Fyn (MAB8900; Millipore), and perforin (2d4; Baetz et al., 1995). Rat antibodies were against LAMP1 (IDB4; Developmental Studies Hybridoma Bank), CD8 (YTS192; provided by H. Waldmann, Oxford University, Oxford, England, UK), granzyme A (7.1; Kramer et al., 1989), granzyme B (C-19; Santa Cruz Biotechnology, Inc.), and CD3 (2C11; BD). Rabbit antibodies against calnexin and actin (Sigma-Aldrich) were used for Western blotting, anti-pERK (9101; Cell Signaling Technology) was used for FACS, and rat anti–LAMP1-PE (IDB4) and CD8α-PerCP-Cy5.5 (53–6.7; BD) were used for the degranulation. Alexa Fluor secondary antibodies (excited at 488, 546, and 633 nm) were obtained from Invitrogen, and HRP-conjugated goat secondary antibodies were purchased from Jackson ImmunoResearch Laboratories, Inc. FACS staining for activation markers was performed with directly conjugated antibodies and isotype-matched controls obtained from eBioscience: anti–mouse CD11a-PE (M17/4), CD25-PE (PC61.5), CD44-PE (IM7), CD62L-PE (MEL-14), CD69–antigen-presenting cell (H1.2F3), CD8a-FITC, and CD8a–antigen-presenting cell (53–6.7).

Cell culture

Lck-inducible mice (Filby et al., 2007) were kept on a doxycycline-supplemented diet from gestation through to adulthood (1 and 3 mg/g) for Lck and Lck/$Fyn^{-/-}$ mice, respectively. Doxycycline was removed 7 d before spleen extraction for Lck^{off} mice. Spleens were disrupted through 40-µm cell strainers (BD), washed twice in serum-free RPMI 1640, and resuspended in complete mouse CTL media [RPMI 1640, 10% FCS, 1% glutamine, 1% sodium pyruvate, 1% kanamycin, 50-µM β-mercaptoethanol, and 100 U/ml IL-2; Roche]) stimulated with either 10^{-7}-M (for F5 WT) or 10^{-6}-M (for Lck^{off}) NP68 peptide (366-ASNENMDAM-374). After 5 d, lymphocytes were purified over Histopaque-1083 (Sigma-Aldrich) and washed twice before further culture in complete medium. H-2^b EL4 target cells were maintained in DME, 10% FCS, and 1% kanamycin. OT-I spleens were activated as F5 but using the ovalbumin peptide (257-SIINFEKL-264; GenScript) at 10^{-8}-M as previously described (Jenkins et al., 2009).

Cytotoxicity assay

CTL cytotoxicity was measured using the CytoTox 96 Non-Radioactive Cytotoxicity Assay (Promega). NP68-pulsed EL4 target cells were incubated in killing assay media (phenol red–free RPMI 1640 and 2% FCS) at 10^5 cells/ml in a round-bottom 96-well plate. CTLs were added to peptide-pulsed EL4 target cells at the ratios shown in Figs. 1 C and 7 A and incubated at 37°C for 4 h. Lactate dehydrogenase release was measured from 50 µl of supernatant, and absorbance was measured at 490 nm. The percentage of target lysis was calculated as (sample target release − target spontaneous)/(maximal release from targets + detergent). All samples were plated in triplicate.

Conjugation of CTLs to targets for immunofluorescence

5×10^5 CTLs and EL4 targets (pulsed with 10^{-3}-M NP68 peptide for 1 h at 37°C and washed three times with media) were in serum-free RPMI 1640 for 5 min before 40-µl aliquots were dropped onto each well of a multiwell slide (CA Hendley) and incubated at 37°C for 20 min. Conjugates were fixed and permeabilized with methanol (precooled to −20°C) on ice for 5 min, washed six times with PBS, and blocked in blocking buffer (PBS and 1% BSA) for ≥30 min at RT. Primary antibodies, diluted in blocking buffer, were incubated for ≥1 h at RT (or overnight at 4°C). Secondary antibodies, diluted in blocking buffer, were incubated for 45 min at RT and washed extensively in blocking buffer and then PBS. Nuclei were stained using 1 µg/ml Hoechst 33342, trihydrochloride, and trihydrate (Invitrogen) in PBS for 5 min at RT and washed in PBS before mounting using 1,4-diazabicyclo[2.2.2]octane (DABCO) mounting media (90% glycerol and 10% PBS + 2.5% DABCO) with No. 1.5 coverslips (Scientific Laboratory Supplies). Conjugates were counted, double blind, by two independent operators.

Fixed images were acquired at RT using either a confocal microscope (510; Carl Zeiss, Inc.) or a spinning-disk confocal system (Revolution; Andor) equipped with Axiovert 200M (Carl Zeiss, Inc.) and IX81 (Olympus) microscopes, respectively, using 100× objectives from the same companies with numerical apertures of 1.4 (Carl Zeiss, Inc.) and 1.45 (Olympus). The spinning-disk confocal system (Revolution) used a 512 × 512, 16 μm^2–pixel camera (iXon; Andor) and a spinning-disk unit (CSU-X1; Yokogawa). Images were acquired using Image Pro (Carl Zeiss, Inc.) or IQ (Andor) software, respectively, and analyzed using an image browser (Carl Zeiss, Inc.) or Volocity (PerkinElmer) and edited using Photoshop software (CS4; Adobe).

EM

CTLs 5–6 d after stimulation were incubated for 15–16 h in 1 mg/ml HRP (Boehringer Ingelheim) in culture medium to load the compartments of the endocytic pathway, including lytic granules. CTLs were washed three times and resuspended in serum-free RPMI 1640 at 10^6 cells/ml and mixed 1:1 with EL4 target cells unpulsed or pulsed with a 10^{-3}-M NP68 peptide. Cells were left in suspension at RT for 5 min and then plated at 0.5 ml of 5×10^5 cells/well in 24-well dishes and incubated at 37°C for either 20, 40, or 60 min. Cells were fixed at RT in 1.5% gluteraldehyde/2% PFA in PBS for 50 min, washed in PBS followed by 0.1-M cacodylate, and processed for DAB cytochemistry as described previously (Stinchcombe et al., 2001). Postfixation procedures with 1% osmium and staining with urynal acetate were performed as previously described (Jenkins et al., 2009). Samples were processed for Epon embedding as previously described (Stinchcombe et al., 2001), thin and semithin sections were stained with lead citrate and viewed using an electron microscope (CM100; Phillips), and images were captured on photographic negative film (Kodak). Negatives were scanned and recorded digitally.

Coating of latex beads with immunoglobulin and CTL conjugation

Sulfated latex (S37230; Interfacial Dynamics Corporation) were diluted and washed twice in 0.1-M MES buffer (M0164; Sigma-Aldrich). 80×10^6 beads/ml were coated with 100 µg/ml of antibody in 0.025-M MES buffer overnight at RT, washed twice in PBS/3% BSA, and pelleted at 3,000 *g* for 20 min. Nonspecific binding was blocked in 1 ml of filter-sterilized PBS/1% BSA for ≥30 min at RT. 20 µl of antibody-coated latex beads was seeded onto multiwell slides in serum-free medium at 10^6 beads/ml for ≥1 h before conjugation. 20 µl CTL (10^6 cells/ml) was added, and conjugates formed for 20 min at 37°C before fixation.

Degranulation analysis by monitoring CD107a presentation

5×10^5 CTLs and 5×10^5 NP68-pulsed EL4 targets were incubated in a round-bottom 96-well plate in a maximum volume of 200 µl mCTL media for 30 min at 37°C in the presence of 2 µg/ml anti–CD107a-PE, washed three times, and resuspended in ice-cold FACS buffer (PBS/0.2% BSA and 0.02% NaN_3) on ice. After the final wash, cells were incubated with 2 µg/ml anti–CD8α-PerCP-Cy5.5 on ice, washed, resuspended in FACS buffer, and analyzed using a FACSCalibur analyzer (BD). Data were analyzed using FlowJo software (Tree Star, Inc.).

In addition to the results shown in Fig. 2 D, Lck^{off} CTLs were tested for degranulation in response to peptide-pulsed or unpulsed targets. Lck^{off} CTLs gave 1.6% LAMP1-positive cells with unpulsed targets and 13.3% with pulsed targets (presumably reflecting the very small amounts of Lck remaining in a small number of cells even after depletion). However, Lck^{off} CTLs nucleofected with Lck-YFP gave 8.9% LAMP1-positive cells with unpulsed targets but 26.1% LAMP1-positive cells with peptide-pulsed targets. WT cells gave 59.3% LAMP1-positive cells in response to peptide-pulsed targets.

Flow cytometry

For analysis of activation markers, CTLs were stained in FACS buffer (PBS and 2% FCS) for 20 min at RT with primary antibodies diluted at 1:100, washed in FACS buffer, and analyzed using a FACSCalibur and FlowJo software. For analysis of ERK activation, 5×10^5 CTLs and 5×10^5 NP68-pulsed EL4 targets were incubated in a round-bottom 96-well plate in a maximum volume of 200 µl mCTL media for 0, 15, and 30 min before 2% PFA fixation and methanol permeabilization (precooled to −20°C). Samples were then immunostained and analyzed as described for degranulation experiments except using anti-pERK primary and goat anti–rabbit Alexa Fluor 488 secondary antibodies. The ERK inhibitor UO126 (Promega) was used throughout the assay at 10 µM, preincubating CTLs for 30 min at 37°C and 5% CO_2 before the assay.

Activation of CTLs using an antibody-coated surface

96-well round-bottom plates were coated with 1 µg/ml anti-CD3 antibodies (145-2C11; BD) in PBS overnight at 4°C, washed, and blocked with PBS/1% BSA for 30 min at RT. 5×10^5 CTLs were added to antibody-coated wells in a maximum volume of 200 µl of culture media.

Western blotting

Cell lysates were prepared in PBS with 2% Triton X-100, 150-mM NaCl, 50-mM Tris-Cl, pH 8.0, 1-mM $MgCl_2$, and complete protease inhibitor cocktail (Roche) with 2×10^7 cells/ml denatured with an equal volume of 2× SDS loading buffer added (Novex Tris-Glycine SDS Sample Buffer; Invitrogen) at 95°C for 10 min. Proteins were separated on a 12% acrylamide gel with rainbow molecular weight markers (GE Healthcare), transferred to a nitrocellulose membrane (Hybond C; GE Healthcare) using the Mini Trans-Blot Cell system (Bio-Rad Laboratories), and washed with PBS-T (PBS/0.02% Tween) before blocking with PBS-T and 5% BSA blocking buffer. Primary antibodies, diluted in blocking buffer, were added at RT for ≥1 h (or overnight at 4°C). Membranes were washed with PBS-T and incubated with an HRP-conjugated secondary antibody in blocking buffer for 45 min. Membranes were then washed and laid onto ECL developing solution (GE Healthcare) or a Visualizer Western Blot Detection kit (Millipore) following the provided protocols. Blots were developed on medical x-ray film (Fujifilm).

Online supplemental material

Fig. S1 shows that F5 WT, Lck^{off}, and Lck^{off} $Fyn^{-/-}$ CTLs express similar levels of cytolytic proteins. Fig. S2 shows ERK activation in F5 CTLs with NP68-pulsed EL4. Fig. S3 shows quantitation of centrosome polarization without 3D reconstruction. Video 1 shows a 3D rotation of centrosome position in F5 WT CTL–target cell conjugates. Video 2 shows a 3D rotation of centrosome position in F5 Lck^{off} CTL–target cell conjugates. Video 3 shows a 3D rotation of actin labeling in F5 WT CTLs conjugated with NP68-pulsed EL4 cells. Video 4 shows a 3D rotation of actin labeling in F5 Lck^{off} CTLs conjugated with NP68-pulsed EL4 cells. Video 5 shows a 3D rotation of talin distribution in F5 WT CTLs conjugated with NP68-pulsed EL4 cells. Video 6 shows a 3D rotation of talin distribution in F5 Lck^{off} CTLs conjugated with NP68-pulsed EL4 cells. Video 7 shows a 3D rotation of centrosome position in F5 Lck^{off} $Fyn^{-/-}$ CTLs conjugated with target cells. Online supplemental material is available at http://www.jcb.org/cgi/content/full/jcb.201008140/DC1.

This work was supported by a grant from the Medical Research Council (MRC) to R. Zamoyska, an MRC studentship to A. Tsun, an Australian National Health MRC postdoctoral fellowship to M.R. Jenkins, and a Wellcome Trust Principal Research Fellowship to G.M. Griffiths.

Submitted: 24 August 2010
Accepted: 25 January 2011

References

Baetz, K., S. Isaaz, and G.M. Griffiths. 1995. Loss of cytotoxic T lymphocyte function in Chediak-Higashi syndrome arises from a secretory defect that prevents lytic granule exocytosis. *J. Immunol.* 154:6122–6131.

Barnard, A.L., T. Igakura, Y. Tanaka, G.P. Taylor, and C.R. Bangham. 2005. Engagement of specific T-cell surface molecules regulates cytoskeletal

polarization in HTLV-1-infected lymphocytes. *Blood*. 106:988–995. doi:10.1182/blood-2004-07-2850

Bellion, A., J.P. Baudoin, C. Alvarez, M. Bornens, and C. Métin. 2005. Nucleokinesis in tangentially migrating neurons comprises two alternating phases: forward migration of the Golgi/centrosome associated with centrosome splitting and myosin contraction at the rear. *J. Neurosci.* 25:5691–5699. doi:10.1523/JNEUROSCI.1030-05.2005

Blanchard, N., V. Di Bartolo, and C. Hivroz. 2002. In the immune synapse, ZAP-70 controls T cell polarization and recruitment of signaling proteins but not formation of the synaptic pattern. *Immunity*. 17:389–399. doi:10.1016/S1074-7613(02)00421-1

Bornens, M. 2008. Organelle positioning and cell polarity. *Nat. Rev. Mol. Cell Biol.* 9:874–886. doi:10.1038/nrm2524

Combs, J., S.J. Kim, S. Tan, L.A. Ligon, E.L. Holzbaur, J. Kuhn, and M. Poenie. 2006. Recruitment of dynein to the Jurkat immunological synapse. *Proc. Natl. Acad. Sci. USA*. 103:14883–14888.

Denny, M.F., B. Patai, and D.B. Straus. 2000. Differential T-cell antigen receptor signaling mediated by the Src family kinases Lck and Fyn. *Mol. Cell. Biol.* 20:1426–1435.

Desai, R.A., L. Gao, S. Raghavan, W.F. Liu, and C.S. Chen. 2009. Cell polarity triggered by cell-cell adhesion via E-cadherin. *J. Cell Sci.* 122:905–911.

Dumont, C., N. Blanchard, V. Di Bartolo, N. Lezot, E. Dufour, S. Jauliac, and C. Hivroz. 2002. TCR/CD3 down-modulation and zeta degradation are regulated by ZAP-70. *J. Immunol.* 169:1705–1712.

Dustin, M.L., S.K. Bromley, Z. Kan, D.A. Peterson, and E.R. Unanue. 1997. Antigen receptor engagement delivers a stop signal to migrating T lymphocytes. *Proc. Natl. Acad. Sci. USA*. 94:3909–3913.

Etienne-Manneville, S., and A. Hall. 2001. Integrin-mediated activation of Cdc42 controls cell polarity in migrating astrocytes through PKCzeta. *Cell*. 106:489–498. doi:10.1016/S0092-8674(01)00471-8

Filby, A., B. Seddon, J. Kleczkowska, R. Salmond, P. Tomlinson, M. Smida, J.A. Lindquist, B. Schraven, and R. Zamoyska. 2007. Fyn regulates the duration of TCR engagement needed for commitment to effector function. *J. Immunol.* 179:4635–4644.

Freiberg, B.A., H. Kupfer, W. Maslanik, J. Delli, J. Kappler, D.M. Zaller, and A. Kupfer. 2002. Staging and resetting T cell activation in SMACs. *Nat. Immunol.* 3:911–917. doi:10.1038/ni836

Geiger, B., D. Rosen, and G. Berke. 1982. Spatial relationships of microtubule-organizing centers and the contact area of cytotoxic T lymphocytes and target cells. *J. Cell Biol.* 95:137–143. doi:10.1083/jcb.95.1.137

Gomes, E.R., S. Jani, and G.G. Gundersen. 2005. Nuclear movement regulated by Cdc42, MRCK, myosin, and actin flow establishes MTOC polarization in migrating cells. *Cell*. 121:451–463. doi:10.1016/j.cell.2005.02.022

Jenkins, M.R., A. Tsun, J.C. Stinchcombe, and G.M. Griffiths. 2009. The strength of T cell receptor signal controls the polarization of cytotoxic machinery to the immunological synapse. *Immunity*. 31:621–631. doi:10.1016/j.immuni.2009.08.024

Kramer, M.D., U. Fruth, H.-G. Simon, and M.M. Simon. 1989. Expression of cytoplasmic granules with T cell-associated serine proteinase-1 activity in Ly-2+(CD8+) T lymphocytes responding to lymphocytic choriomeningitis virus in vivo. *Eur. J. Immunol.* 19:151–156. doi:10.1002/eji.1830190124

Kuhn, J.R., and M. Poenie. 2002. Dynamic polarization of the microtubule cytoskeleton during CTL-mediated killing. *Immunity*. 16:111–121. doi:10.1016/S1074-7613(02)00262-5

Kuhné, M.R., J. Lin, D. Yablonski, M.N. Mollenauer, L.I. Ehrlich, J. Huppa, M.M. Davis, and A. Weiss. 2003. Linker for activation of T cells, zeta-associated protein-70, and Src homology 2 domain-containing leukocyte protein-76 are required for TCR-induced microtubule-organizing center polarization. *J. Immunol.* 171:860–866.

Kupfer, A., and G. Dennert. 1984. Reorientation of the microtubule-organizing center and the Golgi apparatus in cloned cytotoxic lymphocytes triggered by binding to lysable target cells. *J. Immunol.* 133:2762–2766.

Kupfer, A., D. Louvard, and S.J. Singer. 1982. Polarization of the Golgi apparatus and the microtubule-organizing center in cultured fibroblasts at the edge of an experimental wound. *Proc. Natl. Acad. Sci. USA*. 79:2603–2607. doi:10.1073/pnas.79.8.2603

Kupfer, A., G. Dennert, and S.J. Singer. 1983. Polarization of the Golgi apparatus and the microtubule-organizing center within cloned natural killer cells bound to their targets. *Proc. Natl. Acad. Sci. USA*. 80:7224–7228. doi:10.1073/pnas.80.23.7224

Kupfer, H., C.R. Monks, and A. Kupfer. 1994. Small splenic B cells that bind to antigen-specific T helper (Th) cells and face the site of cytokine production in the Th cells selectively proliferate: immunofluorescence microscopic studies of Th-B antigen-presenting cell interactions. *J. Exp. Med.* 179:1507–1515. doi:10.1084/jem.179.5.1507

Lee, K.H., A.D. Holdorf, M.L. Dustin, A.C. Chan, P.M. Allen, and A.S. Shaw. 2002. T cell receptor signaling precedes immunological synapse formation. *Science*. 295:1539–1542. doi:10.1126/science.1067710

Legname, G., B. Seddon, M. Lovatt, P. Tomlinson, N. Sarner, M. Tolaini, K. Williams, T. Norton, D. Kioussis, and R. Zamoyska. 2000. Inducible expression of a p56Lck transgene reveals a central role for Lck in the differentiation of CD4 SP thymocytes. *Immunity*. 12:537–546. doi:10.1016/S1074-7613(00)80205-8

Levy, J.R., and E.L. Holzbaur. 2008. Dynein drives nuclear rotation during forward progression of motile fibroblasts. *J. Cell Sci.* 121:3187–3195. doi:10.1242/jcs.033878

Lovatt, M., A. Filby, V. Parravicini, G. Werlen, E. Palmer, and R. Zamoyska. 2006. Lck regulates the threshold of activation in primary T cells, while both Lck and Fyn contribute to the magnitude of the extracellular signal-related kinase response. *Mol. Cell. Biol.* 26:8655–8665. doi:10.1128/MCB.00168-06

Lowin-Kropf, B., V.S. Shapiro, and A. Weiss. 1998. Cytoskeletal polarization of T cells is regulated by an immunoreceptor tyrosine-based activation motif–dependent mechanism. *J. Cell Biol.* 140:861–871. doi:10.1083/jcb.140.4.861

Martín-Cófreces, N.B., D. Sancho, E. Fernández, M. Vicente-Manzanares, M. Gordón-Alonso, M.C. Montoya, F. Michel, O. Acuto, B. Alarcón, and F. Sánchez-Madrid. 2006. Role of Fyn in the rearrangement of tubulin cytoskeleton induced through TCR. *J. Immunol.* 176:4201–4207.

Negulescu, P.A., T.B. Krasieva, A. Khan, H.H. Kerschbaum, and M.D. Cahalan. 1996. Polarity of T cell shape, motility, and sensitivity to antigen. *Immunity*. 4:421–430. doi:10.1016/S1074-7613(00)80409-4

Nejmeddine, M., V.S. Negi, S. Mukherjee, Y. Tanaka, K. Orth, G.P. Taylor, and C.R. Bangham. 2009. HTLV-1-Tax and ICAM-1 act on T-cell signal pathways to polarize the microtubule-organizing center at the virological synapse. *Blood*. 114:1016–1025. doi:10.1182/blood-2008-03-136770

Palazzo, A.F., H.L. Joseph, Y.J. Chen, D.L. Dujardin, A.S. Alberts, K.K. Pfister, R.B. Vallee, and G.G. Gundersen. 2001. Cdc42, dynein, and dynactin regulate MTOC reorientation independent of Rho-regulated microtubule stabilization. *Curr. Biol.* 11:1536–1541. doi:10.1016/S0960-9822(01)00475-4

Quann, E.J., E. Merino, T. Furuta, and M. Huse. 2009. Localized diacylglycerol drives the polarization of the microtubule-organizing center in T cells. *Nat. Immunol.* 10:627–635. doi:10.1038/ni.1734

Ratner, S., W.S. Sherrod, and D. Lichlyter. 1997. Microtubule retraction into the uropod and its role in T cell polarization and motility. *J. Immunol.* 159:1063–1067.

Ryser, J.E., E. Rungger-Brändle, C. Chaponnier, G. Gabbiani, and P. Vassalli. 1982. The area of attachment of cytotoxic T lymphocytes to their target cells shows high motility and polarization of actin, but not myosin. *J. Immunol.* 128:1159–1162.

Salmond, R.J., A. Filby, I. Qureshi, S. Caserta, and R. Zamoyska. 2009. T-cell receptor proximal signaling via the Src-family kinases, Lck and Fyn, influences T-cell activation, differentiation, and tolerance. *Immunol. Rev.* 228:9–22. doi:10.1111/j.1600-065X.2008.00745.x

Sedwick, C.E., M.M. Morgan, L. Jusino, J.L. Cannon, J. Miller, and J.K. Burkhardt. 1999. TCR, LFA-1, and CD28 play unique and complementary roles in signaling T cell cytoskeletal reorganization. *J. Immunol.* 162:1367–1375.

Stinchcombe, J.C., and G.M. Griffiths. 2007. Secretory mechanisms in cell-mediated cytotoxicity. *Annu. Rev. Cell Dev. Biol.* 23:495–517. doi:10.1146/annurev.cellbio.23.090506.123521

Stinchcombe, J.C., G. Bossi, S. Booth, and G.M. Griffiths. 2001. The immunological synapse of CTL contains a secretory domain and membrane bridges. *Immunity*. 15:751–761. doi:10.1016/S1074-7613(01)00234-5

Stinchcombe, J.C., E. Majorovits, G. Bossi, S. Fuller, and G.M. Griffiths. 2006. Centrosome polarization delivers secretory granules to the immunological synapse. *Nature*. 443:462–465. doi:10.1038/nature05071

Stowers, L., D. Yelon, L.J. Berg, and J. Chant. 1995. Regulation of the polarization of T cells toward antigen-presenting cells by Ras-related GTPase CDC42. *Proc. Natl. Acad. Sci. USA*. 92:5027–5031. doi:10.1073/pnas.92.11.5027

Veillette, A., S. Dumont, and M. Fournel. 1993. Conserved cysteine residues are critical for the enzymatic function of the lymphocyte-specific tyrosine protein kinase p56lck. *J. Biol. Chem.* 268:17547–17553.

Weiss, A., and J.D. Stobo. 1984. Requirement for the coexpression of T3 and the T cell antigen receptor on a malignant human T cell line. *J. Exp. Med.* 160:1284–1299. doi:10.1084/jem.160.5.1284

Zamoyska, R., A. Basson, A. Filby, G. Legname, M. Lovatt, and B. Seddon. 2003. The influence of the src-family kinases, Lck and Fyn, on T cell differentiation, survival and activation. *Immunol. Rev.* 191:107–118. doi:10.1034/j.1600-065X.2003.00015.x